

Study on the Effect of Deep Brain Stimulation Electrode Geometry on Stimulation Range and Discharge Safety Based on COMSOL Muliphysics

Jiahua Li

*School of Physics and Optoelectronic Engineering, Beijing University of Technology, Beijing, China
ljh4305@emails.bjut.edu.cn*

Abstract. Deep Brain Stimulation (DBS) has become a very effective way to treat addiction, depression, and other neurological disorders compared to medications. It stimulates specific areas of the brain through electrodes to regulate various abnormal symptoms. The shape of the electrode affects the discharge range and charge density distribution, which has a great impact on the range of action and safety of the stimulus. Experiments Simulation experiments are performed using COMSOL muliphysics simulation software. By changing the parameters of the position of the electrode terminals and the shape of the electrodes, their discharge behavior is studied. The results showed that the annular electrode with a specific ratio of internal and external radius had a larger stimulation range; a specific upper and lower bottom radius and has better safety performance than truncated cone electrodes. Through the study of the above results, the electrode shape of DBS can be optimized according to clinical needs. By applying these results, the therapeutic effect of DBS can be further improved and a new experimental basis can be provided for the continuous development of brain-computer interaction technology.

Keywords: DBS, Electrode, Shape, COMSOL

1. Introduction

The use of DBS is becoming an effective medical method to treat some conditions like addiction, depression and some neurological disorders. DBS can stimulate the particular part of the human with electrodes, which can give neuron a directly electrical simulation, and solve the disorders with more accuracy and efficacy then traditional drug treatment. Electrodes, as the most direct acting part of DBS technology therapy, should be well designed. Compared with non-invasive electrodes, electrodes that can be implanted in designated areas of the brain can produce clearer signals and stimulate more accurate areas. However, due to the extremely dense brain nerves, if the discharge range of the electrodes is too large, it will lead to unwanted activation of adjacent structures, thereby resulting in dysarthria, sensory dullness and some emotional abnormalities, such as depression, and even induce new epilepsy [1-3]. If the intensity of electrical stimulation is reduced to control the discharge range, the electrical stimulation signal will be insufficient to activate the target area, and the expected therapeutic effect will not be achieved. In addition, prolonged and overly concentrated

electrical stimulation can also cause the solution to be electrolyzed, making the pH and substance concentration unstable, which can cause serious harm to the body [4,5]. There are studies on the optimization of pulse waveforms to address these problems [6]. Experiments show that compared with ordinary square waves, linear falling waves can effectively increase the maximum signal strength that the body can withstand [7]. A study (Shuang F, 2020) demonstrated that nanoporous tungsten as an electrode material can reduce surface impedance and improve signal clarity [8]. At present, the mainstream electrodes on the market are columnar in shape and have segmented contacts [9].

This study begins with a discussion of the theoretical foundations of DBS. First, the principles of DBS are analyzed, examining its components and working processes, and providing examples to explore in detail its mechanisms of action within the brain. Next, by analyzing various parameters of the stimulation signals of DBS, pulse currents that meet the requirements were selected. In the experimental phase, this study utilized COMSOL Multiphysics simulation software to model the discharge behavior of electrodes with different shapes within brain tissue. During the simulation experiment, the researchers first analyzed the electromagnetic equations upon which the software calculations were based, in order to clarify the theoretical foundation of the electrode discharge process. Subsequently, they continuously adjusted the size parameters of the electrodes and the positions of the discharge terminals to alter the shape of the electrodes. By comparing current density distribution to analyze discharge range, and by comparing charge volume density distribution to assess charge injection levels, the scope of the stimulation signals, their clarity, and safety were evaluated.

2. Theoretical foundation analysis

2.1. DBS principle

The basic principle of DBS is to implant electrodes in the vicinity of different targets in the brain, and select high-frequency or low-frequency pulse signals according to specific clinical needs. The electrode applies the electric field of the pulse signal to the targeted area, and the neurons in the abnormal state distributed in this area are interfered with and regulated by the electrical signal, and their neurotransmitter levels are regulated, thereby regulating their lower neural activity or hormone release, so as to achieve the purpose of relieving the patient's symptoms. A common DBS system is shown in Figure 1.

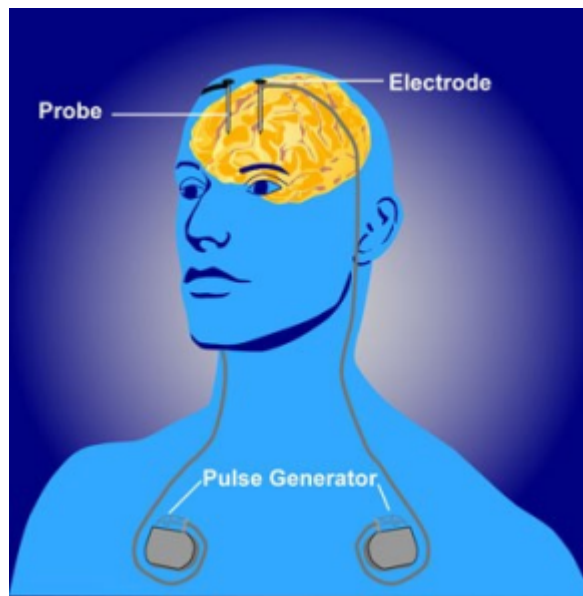


Figure 1. A common DBS system [10]

Take Parkinson's disease (PD), which is widely discussed and most well-used in the field of DBS treatment, as an example: PD is a neurodegenerative disease that can cause slow movement (slowness or inability to move). Clinical symptoms of PD include hand tremors (resting tremor) when relaxed, muscle stiffness, postural balance disorders, etc., in addition, patients may also have non-motor symptoms such as constipation, hyposmia, sleep disorders, autonomic dysfunction and mental disorders. The pathological cause of PD remains unclear at present. The loss of dopamine neurons in the midbrain is an important feature of PD. This directly leads to the failure of the excitatory pathway and the increased effectiveness of the inhibitory pathway in the neural pathways within the basal ganglia, thereby inhibiting the activation of thalamic (TH) neurons. DBS targets the subthalamic nucleus (STN) and implants electrodes to stimulate it with high-frequency pulses, thereby achieving the goal of restoring the activity of TH neurons [11]. During the DBS treatment process, the target cells stimulated are different, and the treatment effects vary greatly. If the discharge range is not limited small enough, it will stimulate the neurons in the inner part of the globus pallidus (GPi). The activation of GPi neurons will inhibit the excitation of TH neurons, thereby affecting the therapeutic effect.

A common DBS device consists of three parts, namely the probe, the extension cord and the pulse generator [12]. The pulse generator is often buried under the collarbone and is powered by a battery. Depending on the treatment needs of different diseases, the severity of the patient's symptoms, and the patient's recovery, the controller placed outside the skin can adjust the intensity, frequency, and width of the pulses. The resulting pulses are delivered via an extension wire to a probe implanted in the target area of the brain to form a complete DBS system.

2.2. Selection of stimulus signals

According to the principle of pulse signal generation of current, it can be divided into two types: the earlier DBS system uses voltage as a stimulus signal to generate current signals in the loop by applying voltage to the body. In a voltage-controlled pulse generator, the strength of the current signal is determined by the impedance within the tissue. Another current current-controlled pulse generator provides a constant current that is not affected by tissue impedance. C. Lettieri's 2015

study showed that current-controlled pulse signals have more stable waveforms than voltage-controlled pulse signals [13].

The parameters of the stimulus signal must be carefully selected: the amplitude of the stimulus signal must be moderate; an amplitude that is too small is difficult to achieve therapeutic effects and is insufficient to activate the target neurons. Excessive amplitude not only leads to a larger activation area, causing neurons to be stimulated unexpectedly and activating the related pathways that cause adverse reactions to form off-target current effects, but also results in a large amount of charge being injected into the tissue, causing electrolysis of tissue fluid and even tissue damage. Adjusting the waveform can mitigate the risk posed by charge injection. Some studies have shown that Gaussian waves or linear descending waves can increase the tissue's tolerance to charge accumulation to a certain extent, but square waves are more widely used at present. The vast majority of DBS solutions today use a two-phase waveform with the goal of approaching zero net injection of charge in a pulse period. Therefore, this square wave should satisfy the following equation:

$$I_1 t_1 = I_2 t_2 \quad (1)$$

Among them, I_1 and t_1 is the absolute value of the amplitude and pulse width of the waveform to stimulate the neurons. I_2 and t_2 is the absolute value of the amplitude and pulse width used to balance the charge.

It is important to note that in treatment, the second waveform of the diphasic waveform to neutralize the charge may hinder the therapeutic effect produced by the first waveform [14]. In Ziheng's 2022 study, it was mentioned that the polarization of membrane potential requires time [15]. Therefore, we can shorten t_2 and extend t_1 to ensure that the target stimulus signal can effectively function. In this paper, the pulse amplitude is selected as $I_1 = 300\mu A$, $I_2 = 3mA$; The width of the pulse is $t_1 = 3ms$, $t_2 = 0.3ms$.

3. Simulation and result analysis

3.1. Simulation settings

In this paper, COMSOL Multiphysics is used to simulate the discharge behavior of electrodes of different shapes within tissues. COMSOL Multiphysics is a powerful multiphysics simulation software that can meet the simulation needs of many scientific research and engineering, including electromagnetism, electrochemistry, structural mechanics, fluid mechanics, thermodynamics, and more. Its rich interface settings and powerful additional modules make it easy to implement modeling and simulation processes [16]. Compared with high-cost and high-risk surgical brain experiments, COMSOL Multiphysics can quickly adjust electrode parameters, quickly obtain electric field data, and avoid the risk of infection caused by surgery.

In this study, a two-dimensional axisymmetric model is used for modeling, and the rotational symmetry of the electrode can greatly simplify the design of the model and optimize the time of software calculation. The Electric Currents (ec) physics field in the AC/DC catalog was selected and studied using the steady-state model. Draw a rectangular simulated brain tissue environment with a width of 300mm and a height of 600mm. Set brain tissue boundaries to 0V (GND). The brain tissue should be set large enough so as to minimize the influence of boundary effects on the experimental data as much as possible. In the conductivity setting, the SC model was selected, and the isotropic conductivity of the white matter of the brain was 0.275S/m. The experimental discharge behavior of

electrodes in columnar, truncated cone, conical shapes (Hereinafter uniformly referred to as columnar) was explored. The diameter of the upper and lower surfaces of the cylinder is set to 0.5mm, which is commonly used for DBS electrodes, and the height is set to 5mm. By constantly reducing the radius of the lower surface, the cylinder can become a cone. The upper surface of the columnar electrode is insulated, and the lower surface and side are set as terminals. The outer diameter of the annular electrode is set to 0.5mm, and the height is set to 5mm. The inner diameter of the annular electrode is changed to compare the discharge behavior of the annular electrode with different inner diameters. The inner surface of the annular electrode is set as the terminal, and the upper and lower bottom surfaces and the outer surface are insulated.

3.2. Simulation experiments

3.2.1. Principles of electromagnetism

Set the terminal current to 300μA as mentioned in 2.2. The simulation software calculates based on the following electromagnetic equations:

$$E = -\nabla V \quad (2)$$

$$J = \sigma E + \mathbf{J}_e \quad (3)$$

$$\nabla \bullet J = Q_{j,v} \quad (4)$$

Among them, \mathbf{E} represents the electric field intensity at each point, V represents the potential at any point, \mathbf{J} represents the current density, $Q_{j,v}$ is the bulk current source density, indicating the current source intensity per unit volume, and σ is the conductivity, \mathbf{J}_e is the density of the applied current. Through these three equations, we can obtain the potential distribution, electric field distribution, current density distribution and spatial accumulation of injected charges in brain tissue.

3.2.2. Simulation of electrode discharge range

The experiment selected 20A/m² as the threshold current density. When the current density modulus at a point in space is greater than the threshold current density, it is considered that the neuron at that point can be activated. It can be intuitively seen from Figure 2, 3, and 4 that as the radius of the lower surface of the columnar electrode decreases, the discharge efficiency of the electrode increases significantly, and the range within which the current density mode is sufficient to activate neurons expands significantly. Let the horizontal distance from the outermost end of the lower surface of the electrode to the threshold current density be the discharge radius.

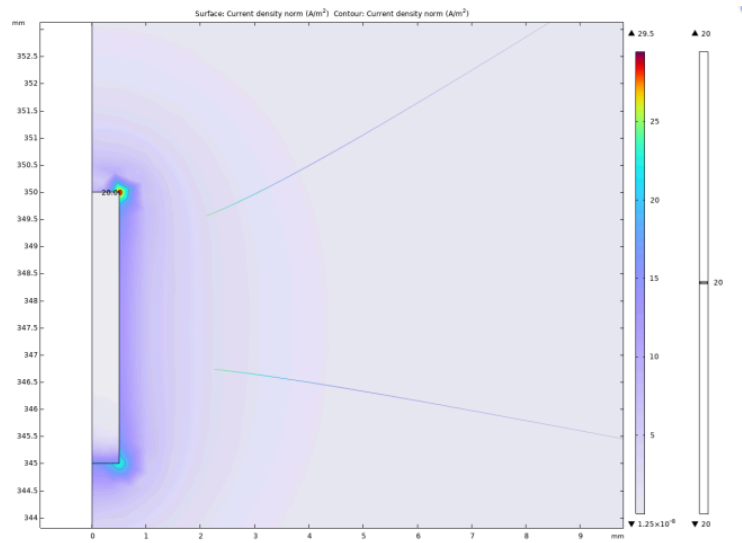


Figure 2. Current density distribution with a bottom radius of 0.5 mm (picture credit: original)

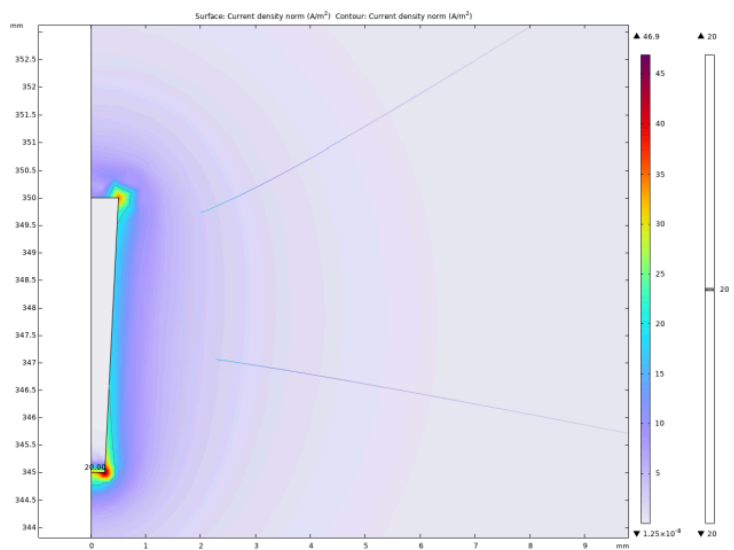


Figure 3. Current density distribution with a bottom radius of 0.25 mm (picture credit: original)



Figure 4. Current density distribution with a bottom radius of 0 mm (picture credit: original)

The experiment shows that when the bottom radius is 0.5mm, the discharge radius is 0.11mm, when the bottom radius is reduced to 0.375mm, the discharge radius increases to 0.17mm, and when the bottom radius is reduced to 0.25mm, the discharge radius increases to 0.19mm. Then the radius of the bottom surface is gradually reduced to 0, and the discharge radius gradually tends to be around 0.21mm. In addition to these results, it can be noted that at the junction of the upper and lower surfaces of the electrodes with the sides, undesired activation zones appear. The activation zones also increase as the radius of the lower bottom of the electrode decreases. As shown in Figs. 5 and 6, the discharge radius of the annular electrode is significantly larger than that of the columnar electrode.

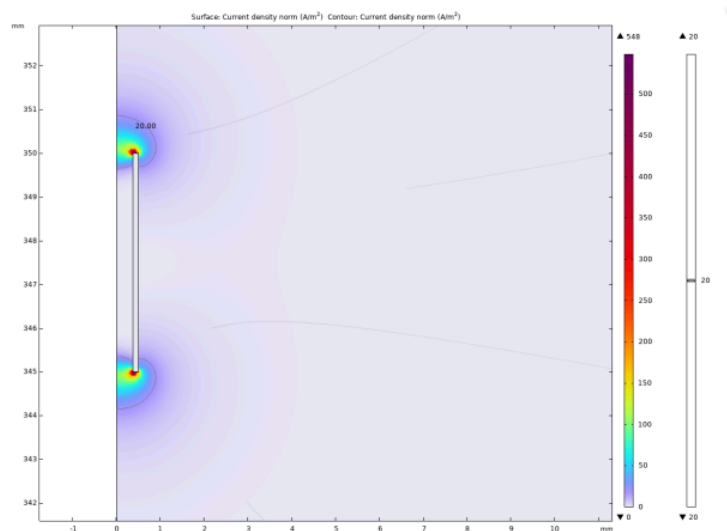


Figure 5. Current density distribution with the inner radius is 0.375mm (picture credit: original)

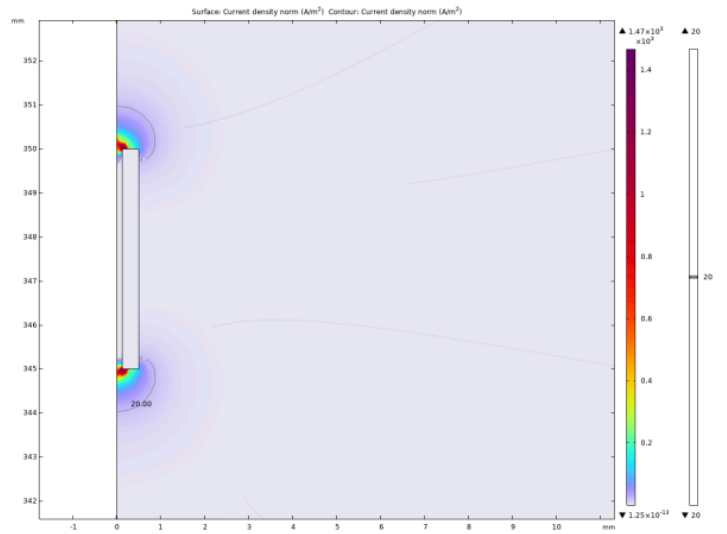


Figure 6. Current density distribution with the inner radius is 0.125mm (picture credit: original)

On the electrode with an inner radius of 0.375mm, the discharge range reaches 0.38mm. When the inner radius is 0.25mm, the discharge range is reduced to 0.35mm. As the inner radius continued to decrease to 0.05mm, there was no significant change in the discharge radius. Considering the difficulty of actual production and the strength of the electrode material, the inner radius is no longer reduced. Similar to the columnar electrode, two activated regions are similarly generated around the annular electrode.

3.2.3. Charge accumulation density analysis

In DBS treatment, accumulated charges can cause electrolysis of brain tissue or other serious damage to the body. Although a dual-phase waveform has been used in the experiment to make the net charge injection within one cycle zero, the amount of charge injected in each single-phase pulse may still cause damage to the organism. Therefore, the smaller the maximum value of charge accumulation density in the experiment, the safer the electrode design.

Table 1. Relationship between maximum bulk charge density and inner radius

r(mm)	0.05	0.1	0.15	0.2	0.25	0.3	0.35	0.4
$\rho(C/m^3)$	0.3061	0.0681	0.0220	0.0050	0.0041	-0.0093	0.0072	0.0104

As shown in Table 1, when the inner radius of the annular electrode is gradually increased starting from 0.05mm, the maximum charge density decreases significantly. The rate of decrease in the maximum charge density gradually slows down. When the inner radius is equal to 0.25mm, the value of the maximum charge density is the smallest. If the inner radius of the electrode is further increased, a negative charge density will be found, and its absolute value will continuously decrease as the inner radius of the electrode increases. In addition, with the appearance of negative charge, the maximum positive charge density begins to rise with the increase of the inner radius.

Table 2. Relationship between maximum bulk charge density and bottom radius

r(mm)	0	0.1	0.2	0.3	0.4	0.5
$\rho(\text{C}/\text{m}^3)$	1.12e-2	4e-3	1.07e-3	4.85e-4	2.72e-4	2.02e-4

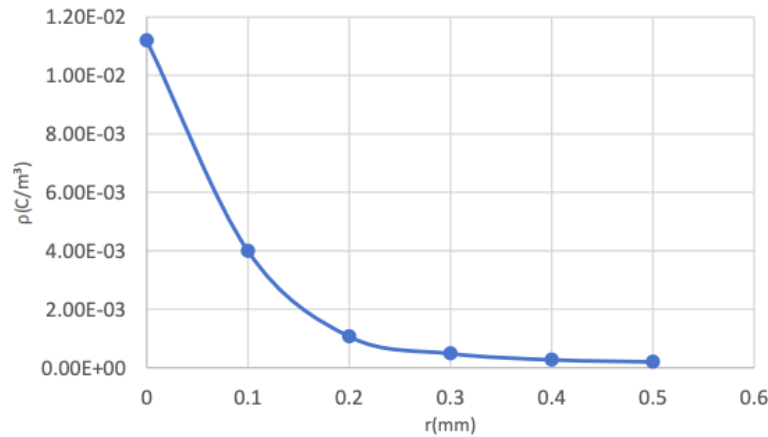


Figure 7. Relationship between maximum bulk charge density and bottom radius (picture credit: original)

It can be known from Table 2 and Figure 7 that the maximum charge density of columnar electrodes is generally lower than that of annular electrodes. As the radius of the base surface increases, the maximum charge density gradually decreases, and the rate of decrease slows down from fast. This means that when the length of the base radius is between 0.3mm and 0.5mm, the safety difference caused by the charge density can be ignored.

3.3. Evaluation of simulation results

Overall, the columnar electrodes discharging on the outer surface of the electrode exhibit a smaller maximum charge density compared to the annular electrodes discharging on the inner surface, which provides a safety advantage. Conversely, the annular electrodes demonstrate higher discharge efficiency and a larger discharge range. When the activation threshold of the target cells is high, requiring more intense stimulation, or when surgical precision is insufficient to place the target cells within the discharge range of the electrode without causing current off-target effects, the annular electrodes may be selected. Experiments indicate that when the ratio of the inner diameter to the outer diameter of the annular electrode is 0.5, safety can be significantly enhanced without affecting the discharge range. When the risk of charge injection is significant, or when there are specific accuracy requirements for the stimulated area, columnar electrodes may be selected. Depending on the requirements of the discharge range, electrodes should be chosen with a lower base radius to upper base radius ratio between 0.6 and 1.

It should be noted that regardless of the shape of the electrode, undesirable activation zones will form near the upper surface. In clinical applications, there exists a certain distance between the upper surface of the electrode and the undesired activated neurons, minimizing the impact of unwanted neuronal activation.

4. Conclusion

Experiments have demonstrated that electrodes of various shapes can be customized to meet different clinical needs. In future research, the experiment will improve the shape of the electrodes to eliminate electrical stimulation near the surface of the electrodes.

Additionally, the experiment will explore the use of porous and roughening techniques on the electrode surface to further optimize the discharge effect of the electrodes. In clinical applications, coatings should also be considered on the surface of the electrodes to improve biocompatibility and reduce damage to brain tissue by electrodes. In order to further ensure safety, we can also design an emergency stop system around the electrodes. By placing sensors in the areas where the charge density is greatest, as calculated by the simulation software, the system will halt discharge if abnormalities in pH or excessive accumulated charge are detected in that location. DBS system will only resume treatment once all parameters near the brain tissue have stabilized.

It is believed that with the continuous optimization of electrodes, the effectiveness and safety of DBS treatment will be greatly improved, and lay a solid foundation for the development of brain-computer interaction technology.

References

- [1] Lange, F., Eldebakey, H., Hilgenberg, A., Weigl, B., Eckert, M., DeSunda, A., Neugebauer, H., Peach, R., Roothans, J., Volkmann, J., & Reich, M. M. (2023). Distinct phenotypes of stimulation-induced dysarthria represent different cortical networks in STN-DBS. *Parkinsonism & Related Disorders*, 109, 105347. <https://doi.org/10.1016/j.parkreldis.2023.105347>
- [2] Chiu, S. Y., Nozile-Firth, K., Klassen, B. T., Adams, A., Lee, K., Van Gompel, J. J., & Hassan, A. (2020). Ataxia and tolerance after thalamic deep brain stimulation for essential tremor. *Parkinsonism & Related Disorders*, 80, 47–53. <https://doi.org/10.1016/j.parkreldis.2020.09.009>
- [3] Olaciregui Dague, K., Witt, J. A., von Wrede, R., Helmstaedter, C., & Surges, R. (2023). DBS of the ANT for refractory epilepsy: A single center experience of seizure reduction, side effects and neuropsychological outcomes. *Frontiers in Neurology*, 14, 1106511. <https://doi.org/10.3389/fneur.2023.1106511>
- [4] Singer, A., Dutta, S., Lewis, E., Chen, Z., Chen, J. C., Verma, N., Avants, B., Feldman, A. K., O'Malley, J., Beierlein, M., Kemere, C., & Robinson, J. T. (2020). Magnetoelectric materials for miniature, wireless neural stimulation at therapeutic frequencies. *Neuron*, 107(4), 631–643.e5. <https://doi.org/10.1016/j.neuron.2020.05.019>
- [5] Kolaya, E., & Firestein, B. L. (2021). Deep brain stimulation: Challenges at the tissue-electrode interface and current solutions. *Biotechnology Progress*, 37(5), e3179. <https://doi.org/10.1002/btpr.3179>
- [6] Gilbert, Z., Mason, X., Sebastian, R., Tang, A. M., Del Campo-Vera, R. M., Chen, K.-H., Leonor, A., Shao, A., Tabarsi, E., Chung, R., Sundaram, S., Kammen, A., Cavaleri, J., Gogia, A. S., Heck, C., Nune, G., Liu, C. Y., Kellis, S. S., & Lee, B. (2023). A review of neurophysiological effects and efficiency of waveform parameters in deep brain stimulation. *Clinical Neurophysiology*, 152, 93–111. <https://doi.org/10.1016/j.clinph.2023.04.007>
- [7] Sahin, M., & Tie, Y. M. (2007). Non-rectangular waveforms for neural stimulation with practical electrodes. *Journal of Neural Engineering*, 4(3), 227–233. <https://doi.org/10.1088/1741-2560/4/3/008>
- [8] Shuang, F., Deng, H., Shafique, A. B., Marsh, S., Treiman, D., Tsakalis, K., & Aifantis, K. E. (2020). A first study on nanoporous tungsten recording electrodes for deep brain stimulation. *Materials Letters*, 260, 126885. <https://doi.org/10.1016/j.matlet.2019.126885>
- [9] Dang, Y., Han, X., & Sun, H., et al. (2025). Technique and accuracy of multi-target intracranial electrode implantation in non-human primates. *Journal of Air Force Medical University*, 46(3), 299–304. <https://doi.org/10.13276/j.issn.2097-1656.2025.03.004>
- [10] Physiopedia. (2023, October 13). Deep brain stimulation. Retrieved August 22, 2025, from https://www.physio-pedia.com/index.php?title=Deep_Brain_Stimulation&oldid=342418
- [11] Singh-Bains, M. K., Waldvogel, H. J., & Faull, R. L. (2016). The role of the human globus pallidus in Huntington's disease. *Brain Pathology*, 26(6), 741–751. <https://doi.org/10.1111/bpa.12429>
- [12] Xiong, B., Zhang, W., & Wang, W. (2024). Deep brain stimulation and brain-computer interface technology: Interdisciplinary convergence of neuroscience, engineering, and clinical medicine. *Journal of Clinical Surgery*, 32(10), 1019–1021.

- [13] Lettieri, C., Rinaldo, S., Devigili, G., Pisa, F., Mucchiut, M., Belgrado, E., Mondani, M., D'Auria, S., Ius, T., Skrap, M., & Eleopra, R. (2015). Clinical outcome of deep brain stimulation for dystonia: Constant-current or constant-voltage stimulation? A non-randomized study. *European Journal of Neurology*, 22(6), 919–926. <https://doi.org/10.1111/ene.12515>
- [14] Lin, Y. (2021). Research on the activation model of DBS pathways in Parkinson's disease [Doctoral dissertation, Harbin Institute of Technology]. CNKI. <https://doi.org/10.27061/d.cnki.ghgdu.2021.002505>
- [15] Zhang, Z. (2022). Regulation of basal ganglia network by improved deep brain stimulation [Doctoral dissertation, Beijing University of Posts and Telecommunications]. CNKI. <https://doi.org/10.26969/d.cnki.gbydu.2022.001878>
- [16] Andras, A., Popescu, F. D., Radu, S. M., Pasculescu, D., Brinas, I., Radu, M. A., & Peagu, D. (2024). Numerical simulation and modeling of mechano–electro–thermal behavior of electrical contact using comsol multiphysics. *Applied Sciences*, 14(10), 4026. <https://doi.org/10.3390/app14104026>